



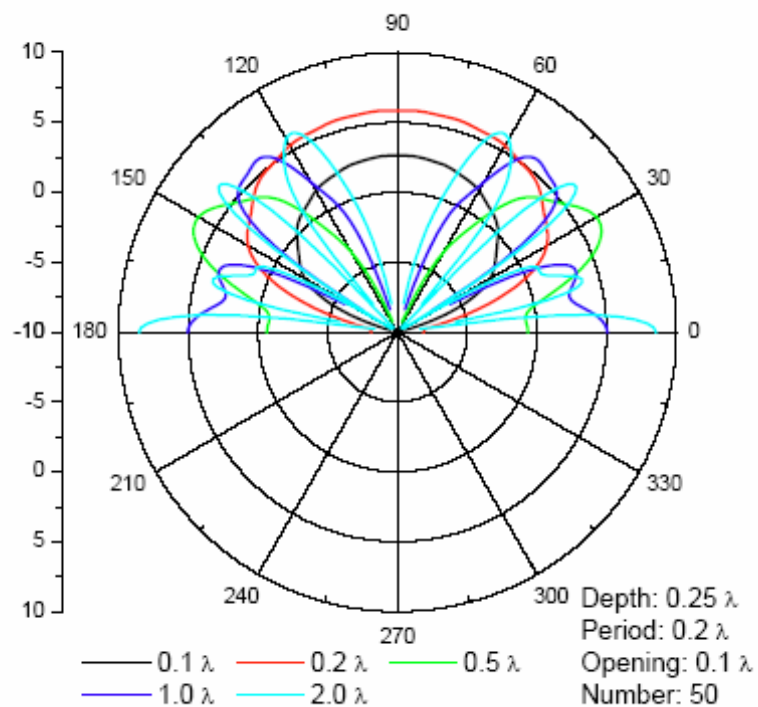
US Army Corps  
of Engineers®

Engineer Research and  
Development Center

## Sound Wave Mitigation Through the Design or Surface Impedance

Weng Cho Chew and Gong Li Wang

August 2005



# Sound Wave Mitigation Through the Design of Surface Impedance

Weng Cho Chew and Gong Li Wang

*Center for Computational Electromagnetics  
Department of Electrical and Computer Engineering  
University of Illinois at Urbana-Champaign  
Urbana, IL 61801-2991*

## Final Report

Approved for public release; distribution is unlimited.

Monitored by: U.S. Army Engineer Research and Development Center  
Construction Engineering Research Laboratory  
Champaign, IL 61822-1076

Under WU#3JD946

**ABSTRACT:** An artificial soft surface is proposed to reduce and attenuate the propagation of acoustic waves along the surface of hard ground. An infinitesimal pressure line source is used as the excitation. Instead of an ideal periodic structure, a quasi-periodic structure is used where a finite number of grooves are incorporated to model exactly the realistic situation. Two boundary integral equation methods are proposed, one is based on the free space Green's function. The multilevel fast multipole algorithm is used to speed up the matrix-vector product necessitated by iterative methods used in solving the final linear system. The second method is more efficient in that two half space Green's functions are employed rather than the free space Green's function so that the edge effect is removed, which results from boundary truncation, and the size of the linear system is greatly reduced. They are then used to analyze the behavior of acoustic wave propagation above textured surfaces, the impedance of which is, as expected, altered. The effects of the number and the geometry of grooves, and the effect of source height are also investigated. The conclusions drawn can be used for reference in a practical problem of mitigating gun blast noise.

**DISCLAIMER:** The contents of this report are not to be used for advertising, publication, or promotional purposes. Citation of trade names does not constitute an official endorsement or approval of the use of such commercial products. All product names and trademarks cited are the property of their respective owners. The findings of this report are not to be construed as an official Department of the Army position unless so designated by other authorized documents.

**DESTROY THIS REPORT WHEN IT IS NO LONGER NEEDED. DO NOT RETURN IT TO THE ORIGINATOR.**

# Contents

List of Figures and Tables .....	iv
Preface.....	vi
I Introduction .....	1
II Physics of Impedance Surface .....	2
III Integral Equation Methods .....	6
IV Effect of Groove Geometry on the Wave Propagation .....	16
V Effect of Source Height on the Radiation Pattern of Power Flow .....	21
VI Conclusion.....	25
References .....	28

## List of Figures

<b>Figure 1</b>	A corrugated surface has low impedance if the grooves are one quarter-wavelength deep and the openings are very small compared to wavelength.....	3
<b>Figure 2</b>	Simple Helmholtz resonators .....	4
<b>Figure 3</b>	Acoustic pressure at (a) a plane hard surface, and (b) a corrugated surface exhibiting high impedance in the lateral direction .....	5
<b>Figure 4</b>	A schematic diagram of a corrugated surface.....	10
<b>Figure 5</b>	Radiation pattern of power flow above a plane rigid surface .....	11
<b>Figure 6</b>	Radiation pattern of power flow above a corrugated surface.....	12
<b>Figure 7</b>	Radiation patterns above a plane surface with different truncated boundaries .....	13
<b>Figure 8</b>	Radiation patterns above a corrugated surface with different truncated boundaries.....	13
<b>Figure 9</b>	Current distribution along the surface for the case in Figure 6 .....	14
<b>Figure 10</b>	Radiation pattern of one groove computed with MLFMA .....	14
<b>Figure 11</b>	Radiation pattern above 50 grooves computed with MLFMA .....	15
<b>Figure 12</b>	Radiation pattern above one groove computed with a new method in which half space Green's function is used instead of free space Green's function .....	15
<b>Figure 13</b>	Radiation pattern above 50 grooves computed with a new method in which half space Green's function is used instead of free space Green's function .....	16
<b>Figure 14</b>	Radiation pattern above corrugated planes with different numbers of grooves.....	17
<b>Figure 15</b>	Radiation pattern above corrugated planes with different groove openings .....	17
<b>Figure 16</b>	A corrugated surface with grooves of different size .....	18
<b>Figure 17</b>	Radiation pattern above a corrugated surface where 50 sets of grooves are used to expand the bandwidth .....	19
<b>Figure 18</b>	Radiation pattern for different heights of source above an idealized hard plane.....	22
<b>Figure 19</b>	The interference of the direct field and the reflected field leads to the nulls and peaks in the radiation pattern.....	22
<b>Figure 20</b>	Radiation pattern for different heights of source above a corrugated surface .....	23

<b>Figure 21</b>	Radiation pattern for different numbers of grooves above a corrugated surface .....	23
<b>Figure 22</b>	Radiation pattern of a higher source above a corrugated surface where the corrugation is of finite extension .....	24
<b>Figure 23</b>	Effective extension of the corrugation .....	24

## Preface

The work was monitored by the Ecological Processes Branch (CN-N) of the Installations Division (CN), Construction Engineering Research Laboratory (CERL). The CERL Principal Investigator overseeing the work was Michael White. This work was done by Principal Investigator Weng Cho Chew and a Research Associate, Gong Li Wang, under Project Number W91321-04-C-0019. Alan Anderson is Branch Chief, CN-N, and L. Michael Golish is Acting Division Chief, CN. The associated Technical Director was William D. Severinghaus, CVT. The Acting Director of CERL is Dr. Ilker Adiguzel.

CERL is an element of the U.S. Army Engineer Research and Development Center (ERDC), U.S. Army Corps of Engineers. The Commander and Executive Director of ERDC is COL James R. Rowan, and the Director of ERDC is Dr. James R. Houston.

## **I. Introduction**

Gun blast noise in military proving grounds has become an environmental pollutant. The environmental noise pollution affects the living quality of people and devalues the land in the vicinity of military proving grounds. A number of studies have been conducted on using various structures to deflect sound wave propagation along the surface of the ground [Swenson *et al*, 1992].

In this research, we suggest the use of impedance surfaces to reduce or attenuate the propagation of sound waves along the surface of the ground. Impedance surfaces have been used recently in microwave to great success [Qian *et al*, 1998]. For microwave, many structures are supported by metallic ground planes. Unfortunately, the metallic ground plane shorts out the electric field, and has the effect of nulling the electric field near the ground plane. This shorting effect makes the radiation of antennas on top of a ground plane inefficient. Recently, new design for surfaces has been suggested that makes a surface appear like an “open circuit” to the electric field. In this manner, the antenna placed on top of a ground plane radiates a lot more efficiently.

In the regime of the present acoustic problem, one expects to achieve the opposite of the above effect. The pressure source leading to noise is assumed situated above a rigid ground; the ground surface is therefore of high acoustic impedance, and thus behaves like an “open circuit” to the acoustic pressure. When a pressure source is located above such a high impedance surface, the image is in phase with itself, thus doubling the pressure in the vicinity of the surface. Henceforth, one needs to lower the surface pressure by changing the high impedance surface into low impedance surface, or by changing the acoustic “open circuit” to acoustic “short circuit”. One possibility of achieving this goal is by texturing the hard surface with a large number of grooves, the geometry of which is carefully chosen so that the surface impedance is assuredly lowered. In the ideal situation, the surface impedance tends to zero and thus appears as a perfect soft surface. For a pressure source above a soft surface, the source image and the source itself are out of phase with each other, then the pressure in the vicinity of the surface is greatly weakened because the image pressure and the pressure from the original source tend to cancel each other in this situation.

The objective of this research is to investigate the application of the artificial soft surface to mitigation of gun blast noise. For the theoretical model to be as close as possible to the real

world problem, a quasi-periodic structure is employed in which a finite number of grooves are included instead of using an infinitely periodic structure. Also an infinitesimal pressure line source is used as the excitation. Plane waves are often used in discussing the behavior of waves above a periodic structure, where the Floquet-Bloch theorem is inevitably used to express the scattered field. It is known that the radiation of a line source can be exactly expressed in terms of the superposition of different plane waves, meaning that the behavior of the line source can be obtained by investigating the behavior of the plane waves. The implementation, however, is not straightforward and there may need to be some approximation [*Lam*, 1999] in doing it this way.

This problem is easily formulated in the form of an integral equation. Generally the free-space Green's function is embedded in the integral to account for the pressure field radiated by the equivalent sources distributed along the surfaces of the ground and the grooves. Since the ground surface extends indefinitely in the horizontal direction, the number of unknowns can be extremely large when the continuous integral equation is discretized. An alternative way is to formulate the problem using two half space Green's functions. In this way, the equivalent sources are only distributed along the opening and the surface of the grooves, hence, the number of unknowns is substantially reduced.

The report is organized as follows. The physical ground of the artificial soft surface is first discussed, which forms the basis for the parameter selection of the groove geometry. Two integral equation methods are then introduced, which are then used to investigate the effects of the number and the geometry of grooves on the propagation of acoustic waves over the quasi-periodic structure. The effect of source height is also addressed. The conclusions are derived from the numerical analysis, which can be used for reference in designing a practical artificial soft surface to suppress the gun blast noise.

## **II. Physics of Impedance Surface**

By incorporating a special texture on an electrically conducting surface, it is possible to alter the electromagnetic properties in microwave frequencies. Likewise, by texturing an acoustically hard surface with a special pattern, the acoustic impedance of the surface can be changed to meet some special requirements raised in practical applications.

The alteration of the surface impedance is generally obtained by embedding a periodic structure in the surface, often called a corrugated surface afterwards. In the regime of electromagnetics, there are various textbooks and papers [Collin, 1990; Kong, 1998; Chew, 2002] dedicated to properties of the corrugated surface. Similar to the definition in electromagnetics, in acoustics a corrugated surface is a rigid plate into which a series of vertical grooves or trenches are cut, as is shown in Figure 1. The grooves are made very narrow, much less than the wavelength

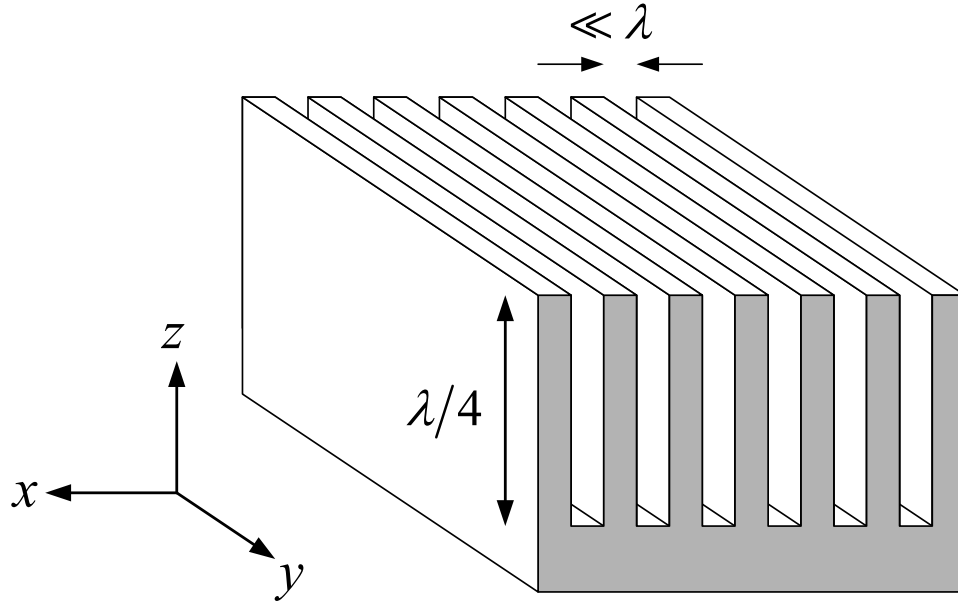


**Figure 1. A corrugated surface has low impedance if the grooves are one quarter-wavelength deep and the openings are very small compared to wavelength.**

of the applied field, so that many of them are fitted within one wavelength. Each groove can be thought of as a parallel-plate transmission line. The bottom of the grooves are electromagnetically open, because the bottom is made acoustically rigid. Therefore, the impedance at the bottom is very high. Inside the grooves, the pressure field can be expanded in terms of waveguide modes

$$p = \sum_{n=0}^{\infty} A_n \cos \left[ \frac{2n\pi}{w} \left( x + \frac{w}{2} \right) \right] \cos [k_{zn} (z + d)], \quad (1)$$

where the vertical component of the wavenumber of  $n$ -th mode is

$$k_{zn} = \sqrt{k^2 - \left( \frac{2n\pi}{w} \right)^2}. \quad (2)$$

Equation (1) holds for  $-w/2 < x < w/2$ . A correct phase shift accounting for wave propagation is needed in Equation (1) for other grooves. As is indicated in Equation (2), when the width of the grooves  $w$  is small enough, only the leading mode is propagating toward the bottom, while others are evanescent. Therefore, if the depth of the grooves is chosen such that it is equal to one-quarter wavelength, the open circuit at the bottom is transformed into a short circuit by the depth of grooves. Thus, the impedance at the top surface of the grooves is very low, and the top surface behaves like a soft surface.

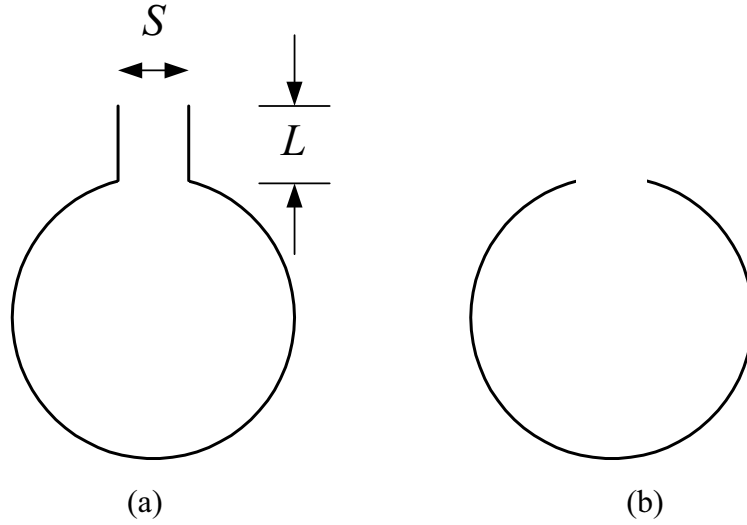


**Figure 2. Simple Helmholtz Resonators.**

In the limit where the wavelength of the applied acoustic field is much larger than the period of the repeating structure, the corrugations can be replaced judiciously with acoustic lumped elements. Here, a simple element of Helmholtz resonator [Kinsler *et al*, 2000] is used to represent each groove, as is shown in Figure 2. As is known that the acoustic impedance of Helmholtz resonator is

$$Z = R + j\left(\omega M - \frac{1}{\omega C}\right), \quad (3)$$

where  $R$  characterizes the radiation resistance,

$$R = R_r / S^2. \quad (4)$$

Here,  $R_r$  is the radiation resistance,  $S$  is the neck area. And  $M$  is its inertance

$$M = m / S^2 = \rho_0 L' / S, \quad (5)$$

where  $L'$  is the effective length of the neck, while  $C$  is its compliance

$$C = S^2/s. \quad (6)$$

Here,  $m$  is the mass of the system and  $s$  is the stiffness. Electrically, this is a series  $RLC$  circuit where  $L$  is the electrical equivalent  $M$ . The system resonates with the applied field at the frequency of

$$\omega_0 = \frac{1}{\sqrt{MC}}. \quad (7)$$

It is known that, at the resonance frequency, the system first absorbs the energy from the pressure source, then radiates the energy into the surrounding media. In the present problem, the system itself does not consume energy, since it is assumed that the inner wall of the system is smooth, so it stores the energy only temporarily and then sends it out totally. The reason that the system, or the grooves, can absorb energy intensively at the resonance frequency is that, at this frequency the surface takes on a low impedance so that the energy can flow in the grooves without difficulty. That immediately means that less energy will flow along the surface. In other words, at other frequencies or when there are no corrugations at the surface, much more energy will flow along the surface to infinity. In terms of impedance, at the resonance frequency, the lateral impedance is higher than when at other frequencies or when the surface is not textured. One expects that, in this scenario, the pressure field attenuates much faster away from the source along the surface, as depicted in Figure 3, which is similar to the field property above an ideal soft surface.

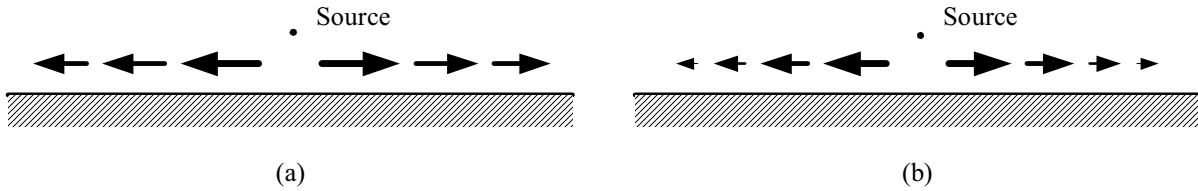


**Figure 3. Acoustic pressure at (a) a plane hard surface, and (b) a corrugated surface exhibiting high impedance in the lateral direction.**

The resonance frequency can also be expressed as

$$\omega_0 = c\sqrt{\frac{S}{L'V}}, \quad (8)$$

Obviously, for a given opening, it is the volume of the cavity, and not its shape, that is important. That means that the resonance frequencies of resonators having the same ratio  $S/L'V$  but having

very different shapes will be found to be identical so long as the wavelength is much larger than any dimensions of the cavity.

The quality factor of the Helmholtz resonator is shown to be

$$Q = 2\pi \sqrt{V \left( \frac{L'}{S} \right)^3}. \quad (9)$$

For a general system as is used in a lot of electromagnetic applications, a high quality factor is preferred. However, since the noise generated by gun blast is of a broad spectrum, a reasonably lower quality factor proves to work better because it is expected to mitigate noise in a frequency range as wide as possible using only one kind of periodic structure. This equation can be used to fine-tune the structure of the grooves to achieve a desired system, which is believed to be a trade-off between the mitigation effect and the quality factor.

### III. Integral Equation Methods

The objective of this research is to investigate the property of acoustic wave above corrugated surface, so as to study the geometry of grooves on the wave propagation. Generally for the problem of this kind, an infinitely periodic structure is used to approximate the practically finite structure and plane wave is used as excitation to study the interaction between the periodic structure and the wave propagating in and above the structure. In the analytical method of this kind, Floquet-Bloch theorem is inevitably used to express the scattered field and the field inside the grooves, thus facilitating the formulation of the problem. The analytical method, however, has some limitations as follows. First, the theoretical infinite model is approximate, and the source can be of finite distribution and can be near the surface; hence, a plane wave is not sufficient to depict its field. For example, the source can be a line source above a one-dimensional periodic structure. It is known that the radiation of a line source can be expressed as the superposition of different plane waves, meaning that the behavior of the line source can be obtained by investigating the behavior of the plane waves. The implementation, however, is not straightforward and there may need to be some approximation [Lam, 1999] in doing it this way. The second is that only when the grooves are of rectangular shape can the field inside grooves be expressed in terms of waveguide modes so that an analytical implementation is applicable. For practical problems such as the present one, the analytical method appears to be limited. This

limitation, however, is readily released when a numerical method is employed, thus allowing for many kinds of groove structures to be investigated.

For the theoretical model to be as close as possible to the real world problem, a quasi-periodic structure is employed in which a finite number of grooves are incorporated instead of using an infinitely periodic structure. Also an infinitesimal pressure line source is used as the excitation so that a two dimensional model is applicable.

Bearing in mind that the ground surface and the inner wall and bottom of the grooves are rigid, a boundary integral equation is suitable to formulate the problem. It is readily obtained as

$$p_{inc}(\mathbf{r}) = \frac{1}{2}p(\mathbf{r}) - \int_{\Gamma} \frac{\partial g(\mathbf{r}, \mathbf{r}')}{\partial n} p(\mathbf{r}') d\Gamma. \quad (10)$$

Here,  $p_{inc}$  is the incident pressure field, and  $p$  is the total pressure field which satisfies

$$\begin{cases} \nabla^2 p(\mathbf{r}) + k^2 p(\mathbf{r}) = -\delta(\mathbf{r} - \mathbf{r}_s) \\ \left. \frac{\partial p(\mathbf{r})}{\partial n} \right|_{\Gamma} = 0 \end{cases}, \quad (11)$$

and  $g$  is the Green's function satisfying

$$\nabla^2 g(\mathbf{r}, \mathbf{r}') + k^2 g(\mathbf{r}, \mathbf{r}') = -\delta(\mathbf{r} - \mathbf{r}'). \quad (12)$$

Note that  $g$  is defined in the whole space or in free space. The symbol  $\Gamma$  represents the uncorrugated surface extending to infinity on both sides and the inner wall and bottom of grooves. The unit vector  $\hat{n}$  is normal to boundary  $\Gamma$ , always pointing to the air from the lower space, or the rigid plate. The factor preceding total pressure  $p$  is from the assumption that  $\Gamma$  is smooth. Otherwise, it is determined by the solid angle made by point  $\mathbf{r}$  with the part of  $\Gamma$  in its vicinity. The rigid boundary condition of  $\partial p / \partial n = 0$  is applied in deriving the integral equation.

The discretization of Equation (10) leads to a complex linear system of the form

$$\mathbf{Ax} = \mathbf{b}. \quad (13)$$

Due to the global behavior of the integral operator, its discrete counterpart,  $\mathbf{A}$  is a dense matrix. When the problem is acoustically large, an iterative method such as the conjugate gradient method (CG) is often invoked to solve for the pressure field along boundary  $\Gamma$ . If direct evaluation of matrix-vector product is used, the computational load for each iteration is  $O(N^2)$ , where  $N$  is the number of unknowns from the discretization. When the problem scale is extremely large, the computational load turns out to be prohibitively large, and a more efficient

algorithm, the multilevel fast multipole algorithm (MLFMA) [Chew *et al*, 2001] can be used to speed up the matrix-vector product. MLFMA allows for the matrix-vector product to be evaluated in operations of  $O(N\log N)$ , a large improvement over the direct multiplication. A computer program based upon MLFMA has already been developed to solve this problem. The use of MLFMA makes it possible to study large problems. For example, it can treat a problem with a large truncated boundary and a large number of grooves.

Note that, in realistic problems, the corrugated surface is distributed only over a finite region; the rest of the surface remains unaltered and extends to infinity on both sides. The following new formulation tries to take advantage of this feature so that the unknowns are distributed only over the corrugated part of the surface, and therefore the number of unknowns is eventually reduced.

Consider two new Green's functions as follows

$$\begin{cases} \nabla^2 g_1(\mathbf{r}, \mathbf{r}') + k^2 g_1(\mathbf{r}, \mathbf{r}') = -\delta(\mathbf{r} - \mathbf{r}') \\ \left. \frac{\partial g_1(\mathbf{r}, \mathbf{r}')}{\partial n_1} \right|_{z=0} = 0, \quad z \geq 0 \end{cases}, \quad (14)$$

$$\begin{cases} \nabla^2 g_2(\mathbf{r}, \mathbf{r}') + k^2 g_2(\mathbf{r}, \mathbf{r}') = -\delta(\mathbf{r} - \mathbf{r}') \\ \left. \frac{\partial g_2(\mathbf{r}, \mathbf{r}')}{\partial n_2} \right|_{z=0} = 0, \quad z \leq 0 \end{cases}. \quad (15)$$

The first Green's function shown in Equation (14) is for the upper space with Neumann condition on fictitious boundary  $z=0$ , and that in Equation (15) is for the lower space with the same condition on the same boundary.

Without loss of generality, we consider a simple case containing only one groove. For convenience, let  $\Gamma_1$  be the points at the boundary  $z=0$ , and  $\Gamma_2$  be the points surrounding the groove, including the points at the opening, the inner wall and bottom of the groove. As is done to derive the integral equation based on the whole space Green's function, using the Green's function for the upper half space, an integral equation is obtained, that is

$$p_{inc}(\mathbf{r}) = p(\mathbf{r}) - \int_{\Gamma_2 \cap \Gamma_1} g_1(\mathbf{r}, \mathbf{r}') \frac{\partial p(\mathbf{r}')}{\partial n_1} d\Gamma, \quad (16)$$

where  $\Gamma_2 \cap \Gamma_1$  is for the points at the opening, and  $\hat{n}_1$  is normal to  $\Gamma_2 \cap \Gamma_1$  pointing from the air to the inside of the groove. Notice that in Equation (16), the factor preceding the pressure  $p(\mathbf{r})$  is

no longer  $1/2$ . This is because for the points at the opening, the source and its image coincide with each other, leading to a new source the intensity of which doubles.

Recalling the integral equation based on the whole space Green's function, or Equation (10), it is interesting to find that now the unknowns are distributed only over the corrugated part of the surface. Considering the opening is much smaller compared to the wavelength, the total number of unknowns will be very small. Notice also that there are two unknown functions, that is, besides the pressure itself, the normal derivative of the pressure is also an unknown function to solve for. However, one of the two unknown functions can be removed using the following Neumann-Dirichlet map.

Applying the second Green's function to the inside of the groove, it is readily obtained for the points at the opening, that

$$0 = p(\mathbf{r}) + \int_{\Gamma_2 \cap \Gamma} p(\mathbf{r}') \frac{\partial g_2(\mathbf{r}, \mathbf{r}')}{\partial n_2} d\Gamma - \int_{\Gamma_2 \cap \Gamma_1} g_2(\mathbf{r}, \mathbf{r}') \frac{\partial p(\mathbf{r}')}{\partial n_2} d\Gamma, \quad (17)$$

and for the points at the wall and bottom of the groove,

$$0 = \frac{1}{2} p(\mathbf{r}) + \int_{\Gamma_2 \cap \Gamma} p(\mathbf{r}') \frac{\partial g_2(\mathbf{r}, \mathbf{r}')}{\partial n_2} d\Gamma - \int_{\Gamma_2 \cap \Gamma_1} g_2(\mathbf{r}, \mathbf{r}') \frac{\partial p(\mathbf{r}')}{\partial n_2} d\Gamma, \quad (18)$$

where  $\Gamma_2 \cap \Gamma$  is for the points at the opening, and  $\hat{n}_2$  is normal to  $\Gamma_2 \cap \Gamma_1$  or  $\Gamma_2 \cap \Gamma$  pointing from the inside of the groove to the outside. Notice in Equation (17) that the factor preceding the pressure  $p(\mathbf{r})$  is also 1, the reason for which is the same as that in Equation (16).

Before proceeding, we first represent the above three equations in the operator form. Equation (16) then becomes

$$p_{inc} = p_{\Gamma_2 \cap \Gamma_1} - \mathcal{L}_1 \frac{\partial p_{\Gamma_2 \cap \Gamma_1}}{\partial n_1}, \quad (19)$$

and Equations (17) and (18) become

$$0 = p_{\Gamma_2 \cap \Gamma_1} + \mathcal{L}_C p_{\Gamma_2 \cap \Gamma} - \mathcal{L}_D \frac{\partial p_{\Gamma_2 \cap \Gamma_1}}{\partial n_2}, \quad (20)$$

$$0 = \left( \mathcal{L}_A + \frac{1}{2} \mathcal{I} \right) p_{\Gamma_2 \cap \Gamma} - \mathcal{L}_B \frac{\partial p_{\Gamma_2 \cap \Gamma_1}}{\partial n_2}. \quad (21)$$

From these equations, it is found that

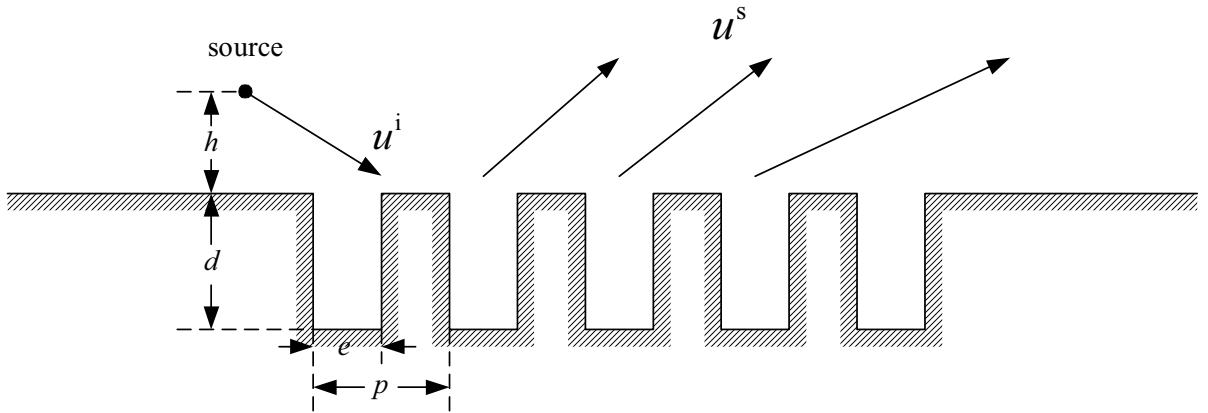
$$p_{inc} = (\mathcal{L}_1 + \mathcal{L}_2) \frac{\partial p_{\Gamma_2 \cap \Gamma_1}}{\partial n_2}, \quad (22)$$

where

$$\mathcal{L}_2 = \mathcal{L}_D - \mathcal{L}_C \left( \mathcal{L}_A + \frac{1}{2} \mathcal{I} \right)^{-1} \mathcal{L}_B \quad (23)$$

is the Neumann-Dirichlet map as mentioned above, which maps the normal derivative of the pressure to the pressure itself at the opening of the groove. Equation (22) is the final equation that we are going to solve. Compared to that based on the whole space Green's function, or Equation (10), it is found that there is only one unknown function which is distributed only over the opening of the groove, the number of discrete unknowns being reduced substantially.

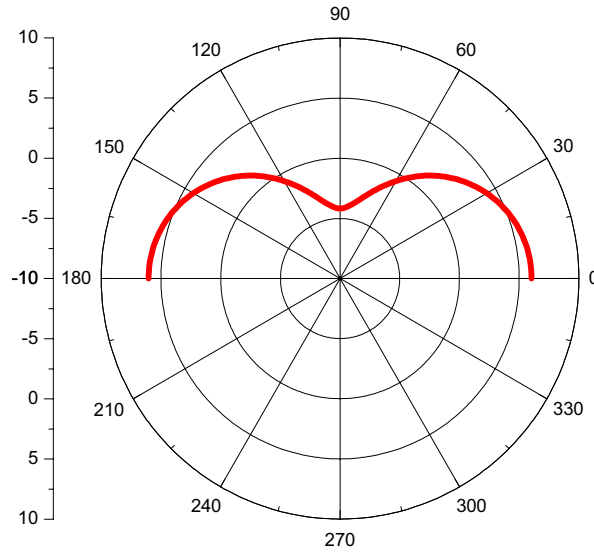
The Neumann-Dirichlet map, after discretization, turns into an impedance matrix. Suppose that in discretization, the element number along the opening is  $N$ , and the number along the inner wall and the bottom is  $M$ , then the impedance matrix is an  $N \times N$  matrix. The computational amount for the impedance matrix is  $O(M^3 + M^2N + MN^2)$ . Generally  $N$  is much smaller than  $M$ , then the computational amount is approximately  $O(M^3)$ , coming basically from the evaluation of the inverse of  $\mathcal{L}_A + \mathcal{I}/2$ . For a quasi-periodic structure, only one inverse evaluation is necessary because generally all grooves are of the same geometry. For the worse case where all the grooves are of different shape, inverse evaluation is needed for each groove. Still the entire computation is efficient because the grooves are acoustically small, and therefore the associated impedance matrices are small. The inverse of the impedance matrices is calculated



**Figure 4. A schematic diagram of a corrugated surface.**

using Gauss-Jordan elimination. For the final reduced linear system, one may use a direct solver. However, the conjugate gradient method is used in our computations.

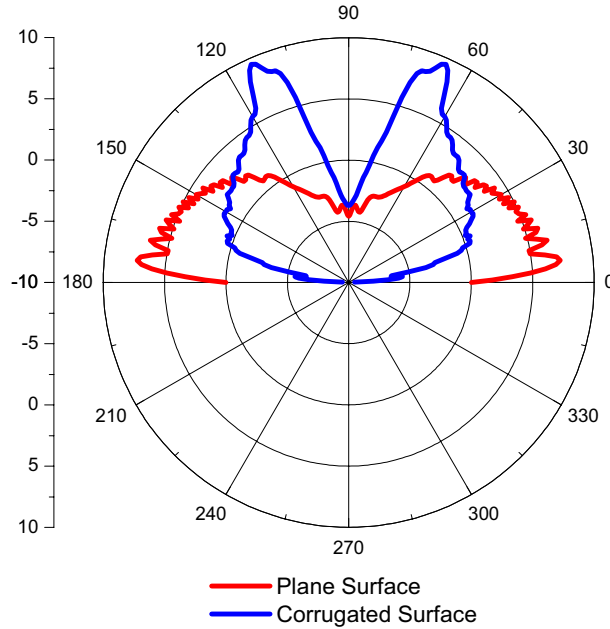
Now we proceed to validate the MLFMA and the new method against analytical method where available, and a direct solver using Gaussian elimination. The corrugated surface to be used is in Figure 4. In the first case, the source is located  $0.2\lambda$  above the surface. The groove opening and depth are  $1\lambda$  and  $2\lambda$  respectively. There are totally 20 grooves cut into the surface. When there is no corrugation, the radiation pattern of power flow is shown in Figure 5, which is calculated analytically. For a rigid plane, the source and its image are in phase with each other, and the two fields superimpose constructively in the vicinity of the surface, as is seen in the figure. Only a half circle is given, since the radiation is limited to the upper half space.



**Figure 5. Radiation pattern of power flow above a plane rigid surface.**

When MLFMA is used in practical computation, the infinitely extending surface is truncated at both sides, so there will exist an edge effect if the truncated surface is not large enough. In such a situation, the wave travels along the surface till the two ends of the surface are encountered, and then it radiates into the space, leading to ripples at the radiation pattern. The most appreciable ripples occur near the surface, as is depicted by red line in Figure 6. As a practical way to overcome this problem, the radiation pattern of a truncated plane surface is computed and is compared with that of a truncated corrugated surface. The comparison is therefore reasonable since both radiation patterns contain the same edge effect. As an application,

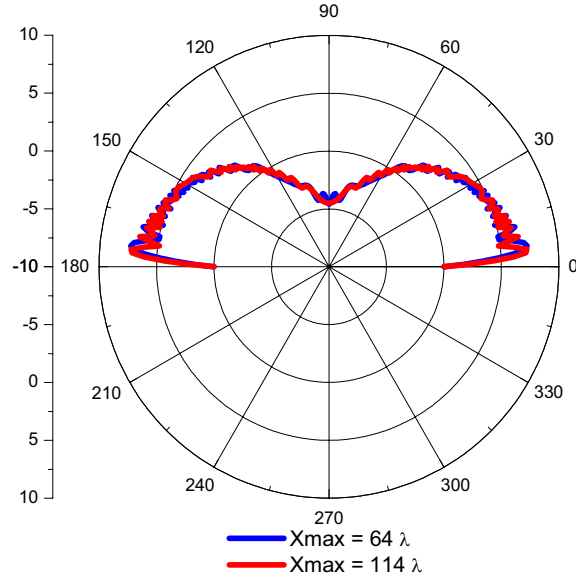
Figure 6 shows the radiation pattern above the corrugated surface against that above the plane surface computed numerically with the same truncated boundary.



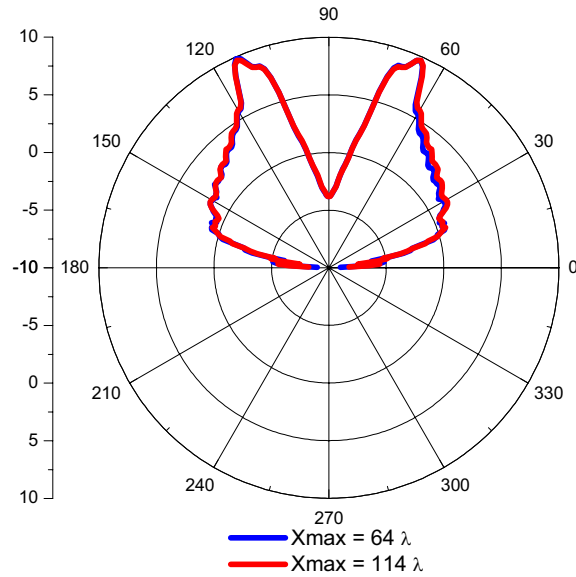
**Figure 6. Radiation pattern of power flow above a corrugated surface.**

Figure 6 is obtained by truncating the plane at a distance of  $64\lambda$  from the source. Now it is truncated at a distance of  $114\lambda$ , and the radiation pattern above the plane surface is shown in Figure 7, while the radiation pattern above the corrugated surface is shown in Figure 8. It can be seen that increasing the truncated boundary has almost no effect on the result in Figure 8, while the result in Figure 7 tends to the radiation pattern for an infinite plane surface. In Figure 9 it is seen that the magnitude of pressure at the two ends of the corrugated surface is about one fifth that of the plane surface, explaining why the radiation pattern in Figure 8 is almost not affected. It means that the truncated boundary at a distance of  $64\lambda$  is large enough in this case.

Figure 9 also shows that the analysis associated with Figure 3 is reasonable. Figures 3 and 9 are actually saying the same thing, that is, by choosing suitable geometric parameters of grooves, the surface may show high acoustic impedance in the lateral direction, thus suppressing the acoustic wave propagating along the surface.



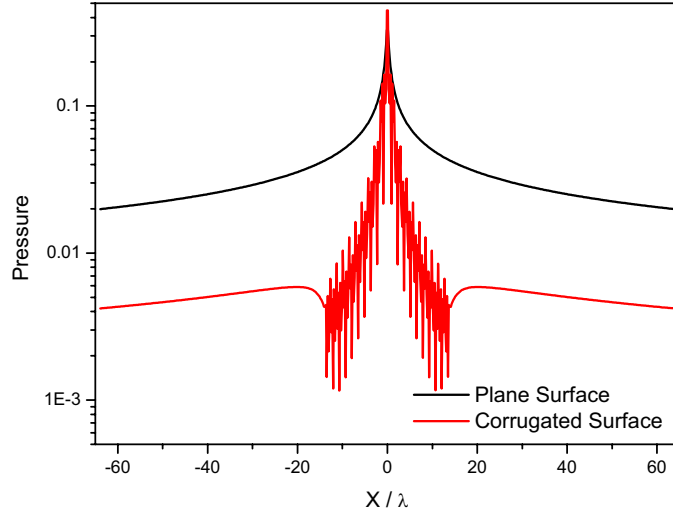
**Figure 7. Radiation patterns above a plane surface with different truncated boundaries.**



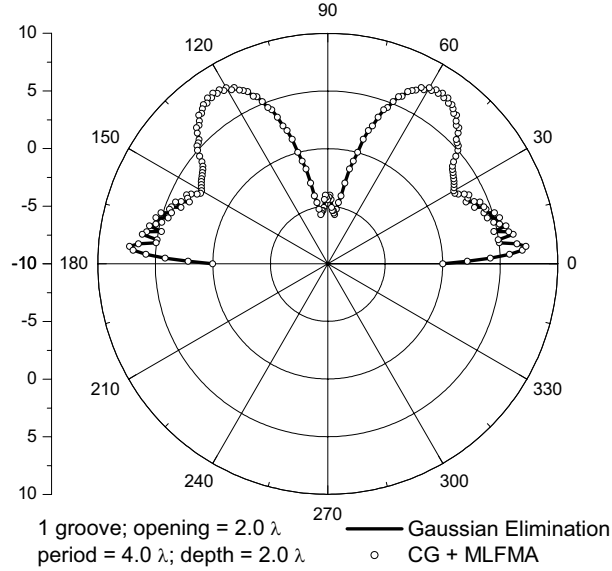
**Figure 8. Radiation patterns above a corrugated surface with different truncated boundaries.**

Figure 10 shows the radiation pattern over a corrugated surface computed with MLFMA and its comparison with the direct solver. The agreement is excellent. One groove is included in this model. The geometry is given in the figure. The source is  $0.2 \lambda$  above the corrugation. In the

following, the source height is always the same without specification. Figure 11 shows the radiation pattern above 50 grooves computed with MLFMA. The black line is obtained by using the direct solver. Excellent agreement is observed between the two results.



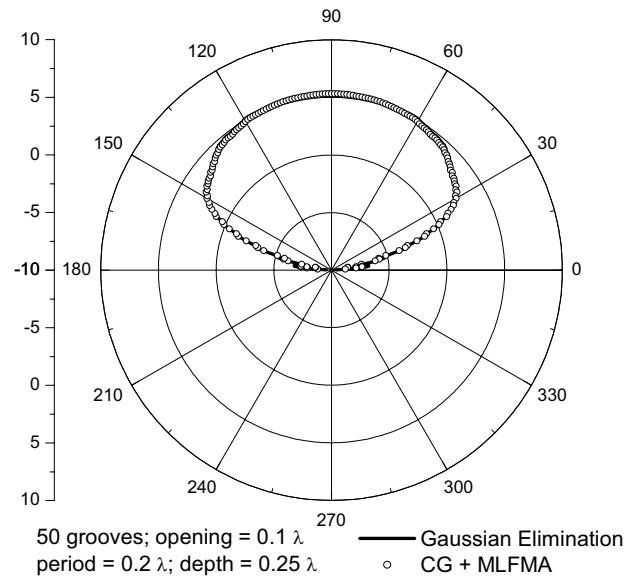
**Figure 9. Current distribution along the surface for the case in Figure 6.**



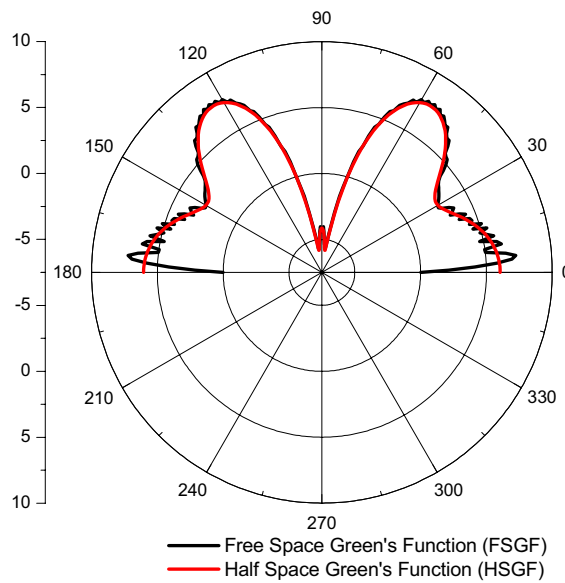
**Figure 10. Radiation pattern of one groove computed with MLFMA.**

In MLFMA and the director solver, free space Green's function is used. Therefore, as indicated above, edge effect is always involved in computations, though sometimes it is

negligible. To suppress the edge effect, a large truncated boundary is necessary, which unfavorably increases the number of unknowns, thus slows down the code execution.

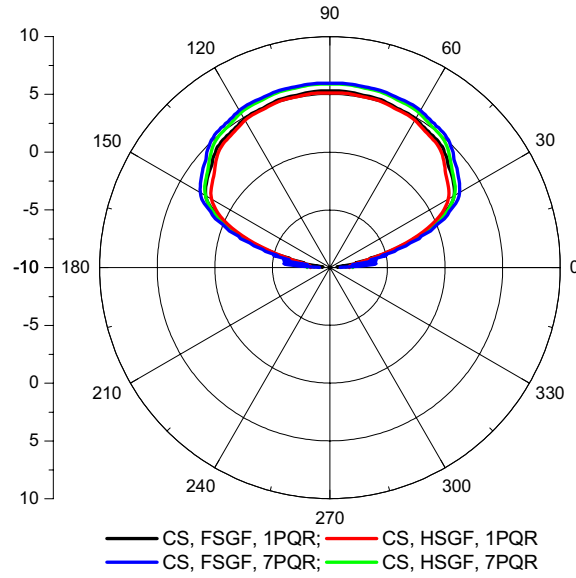


**Figure 11. Radiation pattern above 50 grooves computed with MLFMA.**



**Figure 12. Radiation pattern above one groove computed with a new method in which half space Green's function is used instead of free space Green's function.**

Figure 12 shows the radiation pattern over a corrugated surface computed with the new method. The geometry of the corrugated surface is the same as Figure 10. It is seen that the small oscillations over the radiation pattern in Figure 10 totally vanish, which has been shown to come from the interference of the radiation from the two ends of truncated surface. The radiation pattern computed using the new method is clearly smooth and the inward deflection near the surface is eliminated.



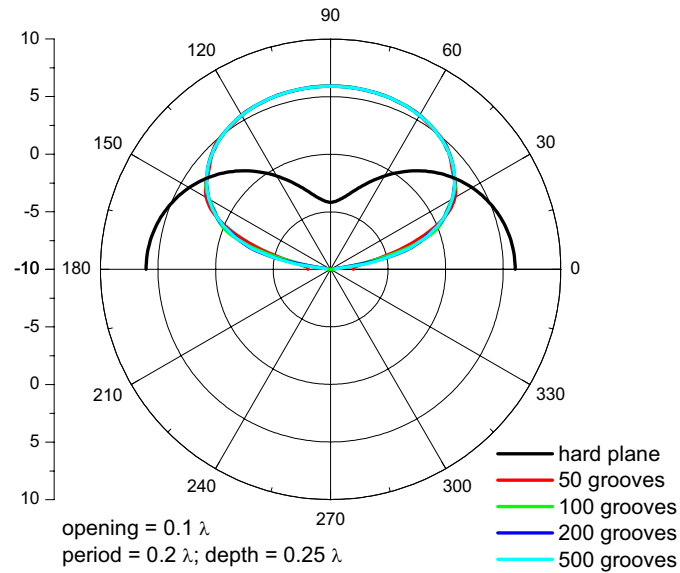
**Figure 13. Radiation pattern above 50 grooves computed with a new method in which half space Green's function is used instead of free space Green's function.**

Figure 13 shows the radiation pattern above 50 grooves computed with the new method. Because the openings are very small compared to the wavelength, some elements may be very close to each other. To examine the effect, two kinds of trapezoidal quadrature rules are used, the first is one point, and the second is seven points. It is seen that the result changes, though slightly, when different quadrature rules are used. This implies that one needs to exercise caution when openings are very small.

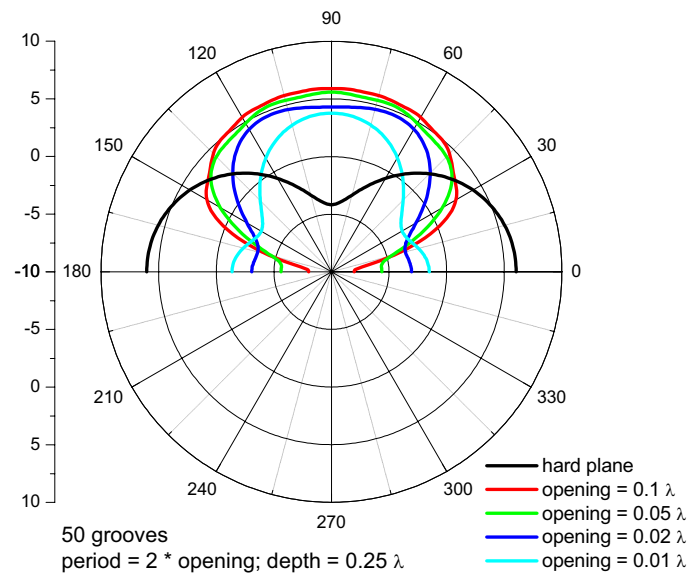
#### IV. Effect of Groove Geometry on the Wave Propagation

Figure 14 is to investigate the effect of number of grooves on the radiation pattern. It is seen that when the number increases, the pattern tends more closely to the ideal pattern above a

soft surface. However, generally, only small discrepancies are observed between the results shown in the figure. This is of practical importance, meaning that it is not necessary to use a very large number of grooves.



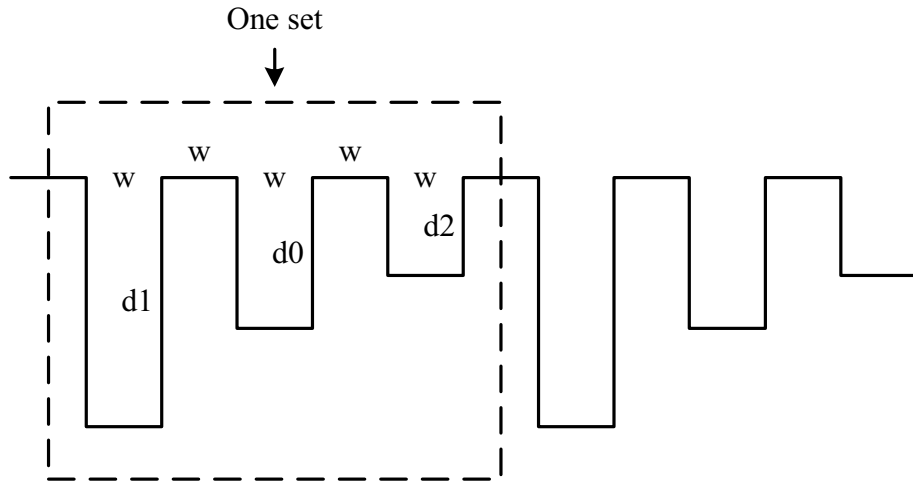
**Figure 14. Radiation pattern above corrugated planes with different numbers of grooves.**



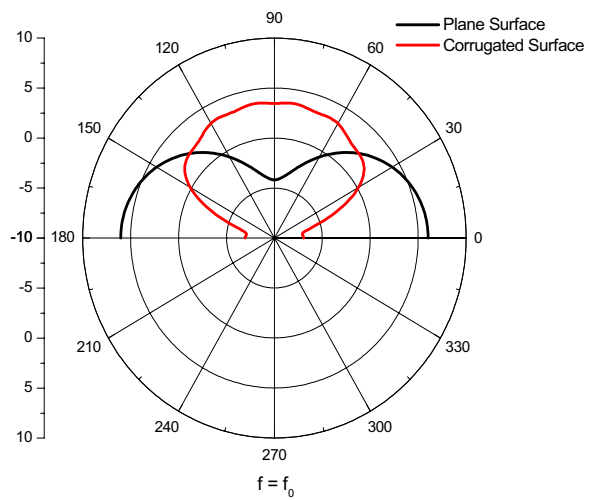
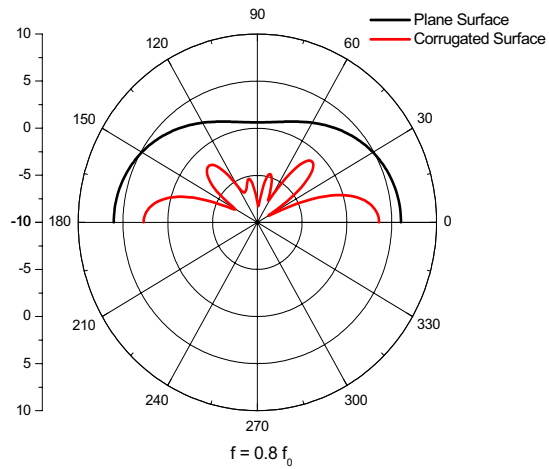
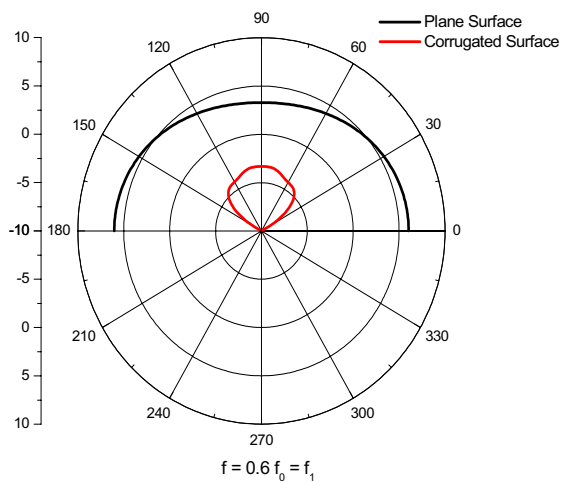
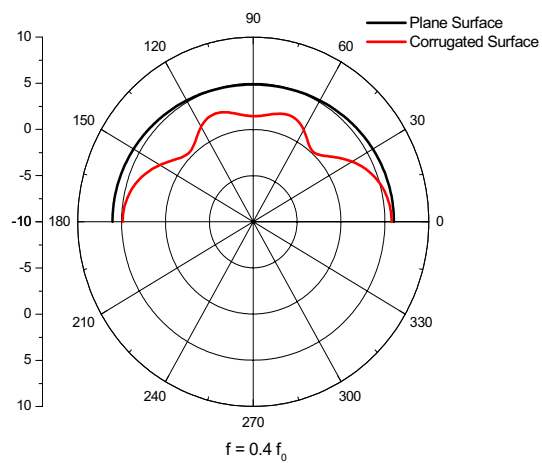
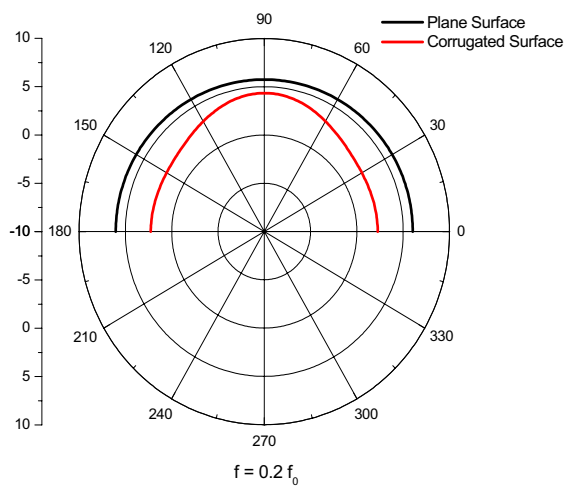
**Figure 15. Radiation pattern above corrugated planes with different groove openings.**

Figure 15 is to investigate the effect of groove openings on the radiation pattern. Because the number of grooves is fixed for different openings, we see that the effect of mitigation in grazing direction is weakened. If the central frequency to be suppressed is 50Hz, then  $0.1\lambda$  is about 70 centimeters, too large to be practical. Therefore, decreasing the openings is also of practical importance. A possible method to balance the weakening effect may be increasing the number of grooves.

Another problem of concern is that the mitigation effect is sensitive to the frequency. A direct way is to use grooves of different size in the same model. As a preliminary test, we propose to use three grooves with the same openings, but with different depths, as shown in Figure 16. Suppose the frequency to be suppressed is from 10 to 90Hz, and the central frequency is 50Hz. Let  $f_0 = 50\text{Hz}$ ,  $f_1 = 30\text{Hz}$ ,  $f_2 = 70\text{Hz}$ , then  $\lambda_1 = 1.667\lambda_0$ ,  $\lambda_2 = 0.714\lambda_0$ . Note that the openings ( $0.02\lambda_0$ ) and period ( $0.04\lambda_0$ ) are very small; the 31-point trapezoidal quadrature rule is used to ensure enough accuracy in interaction computations. Radiation pattern is computed at nine frequency points evenly spaced, viz.,  $0.2f_0$ ,  $0.4f_0$ ,  $0.6f_0$ ,  $0.8f_0$ ,  $1.0f_0$ ,  $1.2f_0$ ,  $1.4f_0$ ,  $1.6f_0$ ,  $1.8f_0$ , and the results are shown in Figure 17. Generally, it can be seen that the use of different grooves indeed expands the bandwidth of forbidden frequency. The source height in this example is  $0.2\lambda_0$ .



**Figure 16. A corrugated surface with grooves of different size. Here,  $d_1 = 0.25\lambda_1$ ,  $d_0 = 0.25\lambda_0$ ,  $d_2 = 0.25\lambda_2$ ,  $w = 0.02\lambda_0$ .**



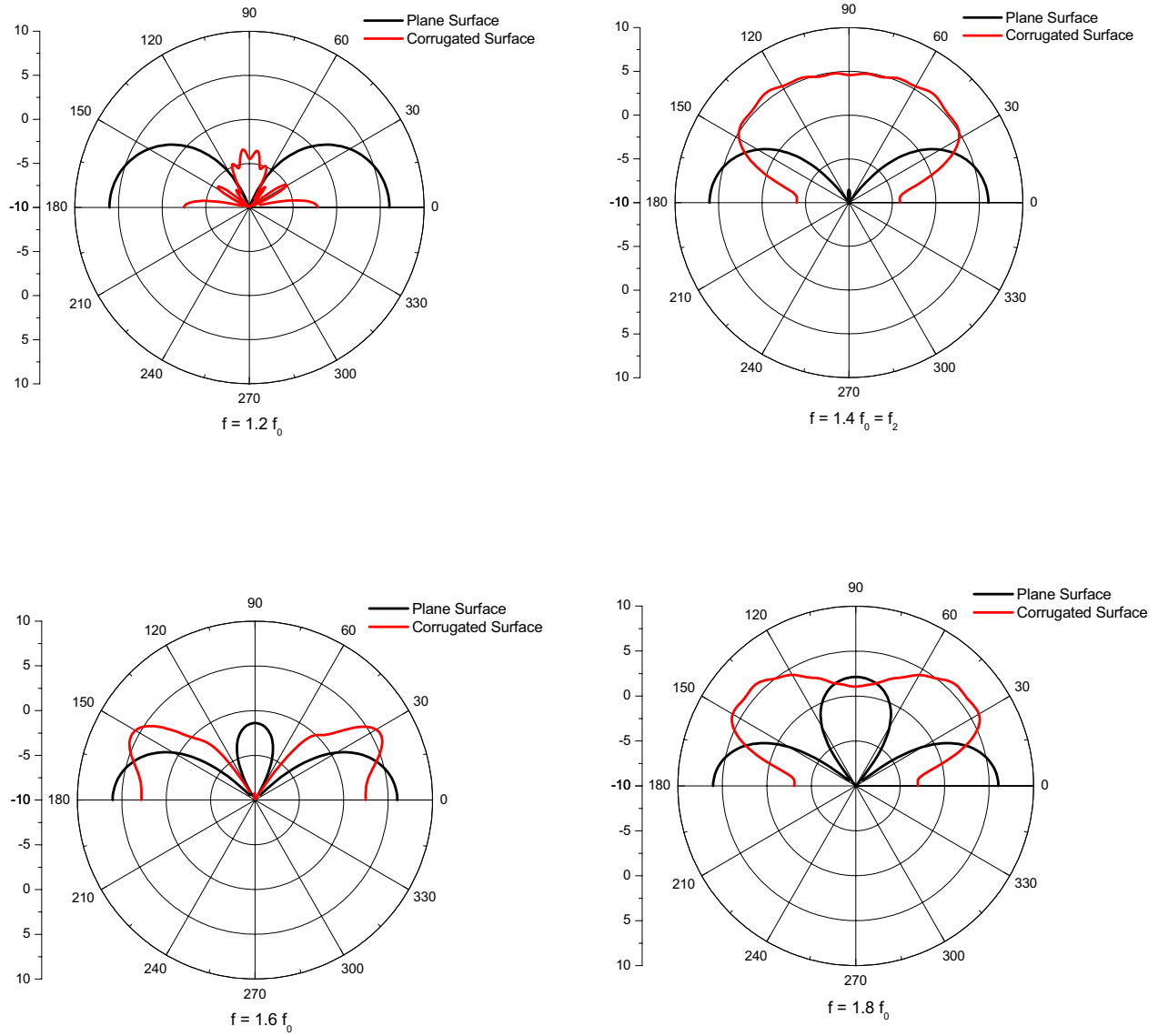


**Figure 17. Radiation pattern above a corrugated surface where 50 sets of grooves are used to expand the bandwidth.**

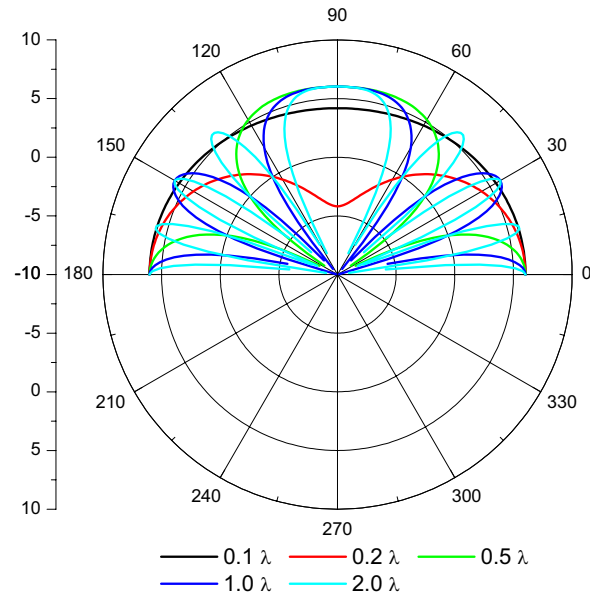
The other way is to use a groove with a narrow neck and a large cavity, that is, a structure like a kettle, which, according to the prediction from Helmholtz resonator, can lower the quality factor, and so is able to expand the forbidden band. This will be a subject of possible future research.

## V. Effect of Source Height on the Radiation Pattern of Power Flow

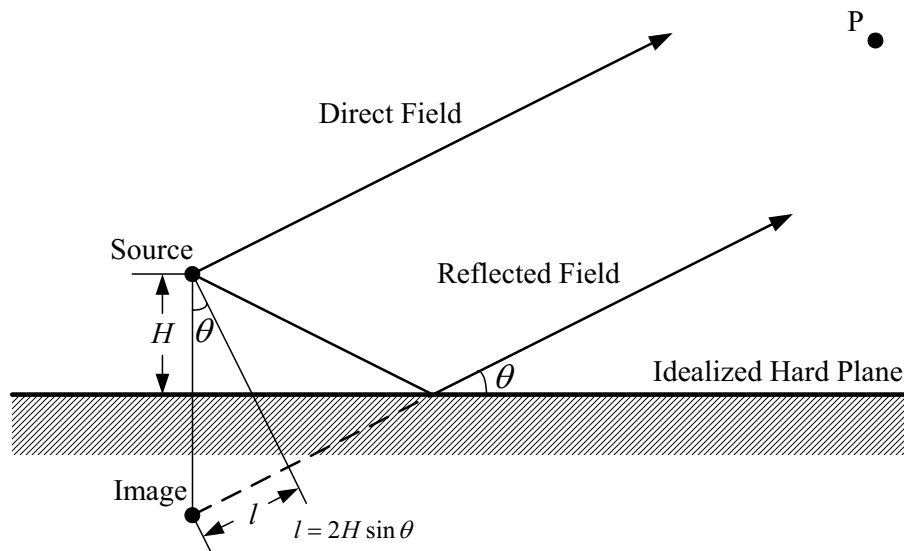
Shown in Figure 18 is the radiation pattern for different heights of source above an idealized hard plane. The most salient feature is that more nulls and peaks are taking place with the increase of the source height. The peak values, however, are kept the same. It is readily explained by the image theory, as is shown in Figure 19. The radiated field above an idealized hard plane is the direct field generated by the original source plus the reflected field generated by its image. For a distant point, the field vectors pointed from the two sources are judiciously considered to be parallel to each other. The phase difference is therefore  $2H\sin\theta$ , where  $H$  is the source height, and  $\theta$  is the elevation angle. Due to the existence of the phase difference, the two fields interfere with each other. The radiation pattern is then  $2\cos(2H\sin\theta)$  after being normalized to that of the free space. It is seen that in this case  $H$  plays a role similar to the wave number in the polar direction; hence the larger  $H$ , the more complicated the radiation pattern.

Figure 20 shows the radiation pattern above a corrugated surface. The corrugation is formed by cutting 50 grooves into a plane surface. As in the above case, the higher the source height, the more complicated the radiation pattern. The important thing is that the radiation intensity in the lateral direction becomes larger with the increase of the source height. In other words, the corrugated surface no longer functions as a soft surface for a large source height. This is undesirable. However, by changing the number of grooves, the radiation pattern is expected to be improved. Shown in Figure 21 is the variation of the radiation pattern of a source  $2\lambda$  above the surface with the number of grooves. Here,  $2\lambda$  is the largest height in Figure 20. It is seen that increasing the number of grooves indeed improves the radiation pattern in the lateral direction. In fact, the radiation pattern corresponding to 2000 grooves is very close to that above an idealized soft plane.

The reason is explained as follows. As is shown in Figure 22, the reflection point is defined as the intersection of the field vector from the image source and the ground surface. For the same elevation angle, the higher the source, the larger the distance of the reflection point. Intuitively, when the extension of grooves is larger than the reflection point distance, the corrugated surface behaves as a soft surface. Otherwise, it is too small for the surface to be an artificial soft surface. This means that, for the source of large height, the extension of grooves needs to be larger so that it still behaves like a soft surface. Note that, in Figure 21, for higher elevation angles, the radiation intensity is almost not affected by the number of grooves, only



**Figure 18. Radiation pattern for different heights of source above an idealized hard plane.**



**Figure 19. The interference of the direct field and the reflected field leads to the nulls and peaks in the radiation pattern.**

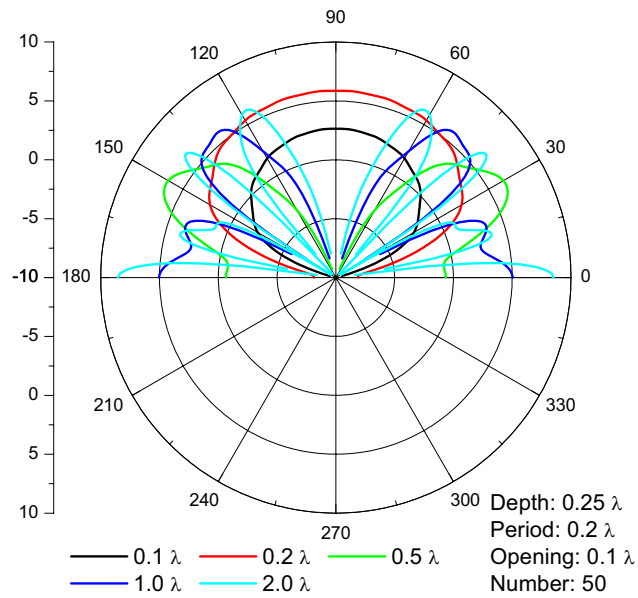


**Figure 20. Radiation pattern for different heights of source above a corrugated surface.**

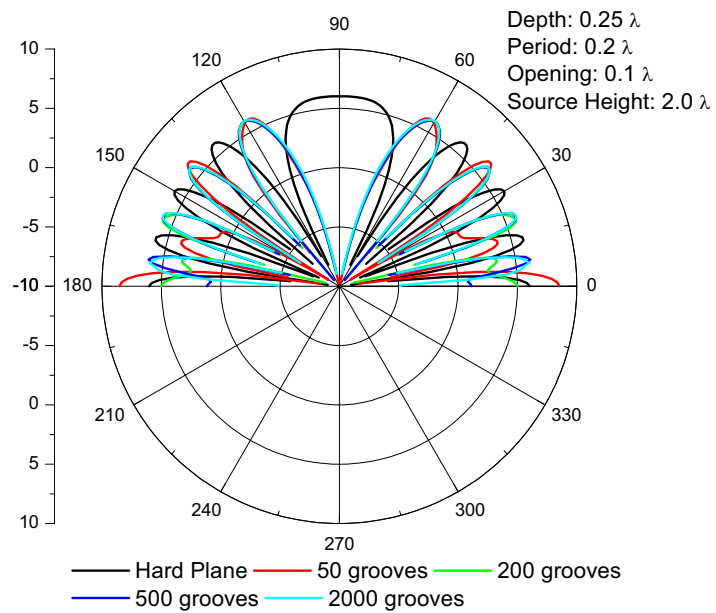


**Figure 21. Radiation pattern for different numbers of grooves above a corrugated surface.**

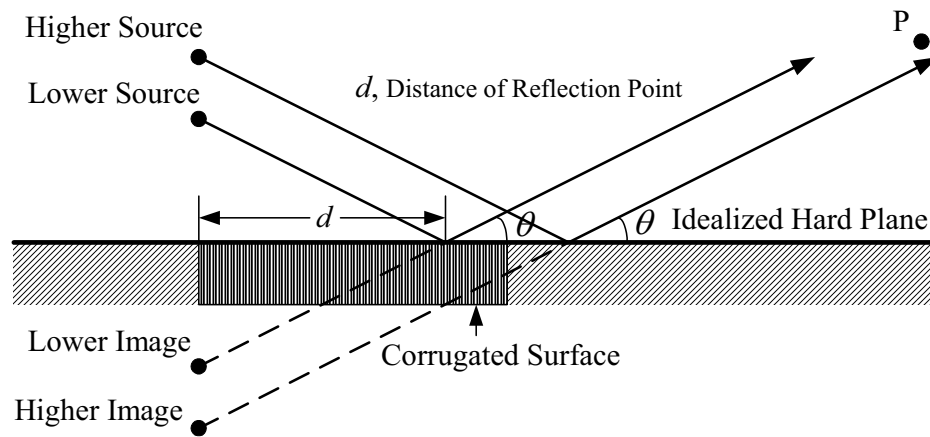


**Figure 22. Radiation pattern of a higher source above a corrugated surface where the corrugation is of finite extension.**

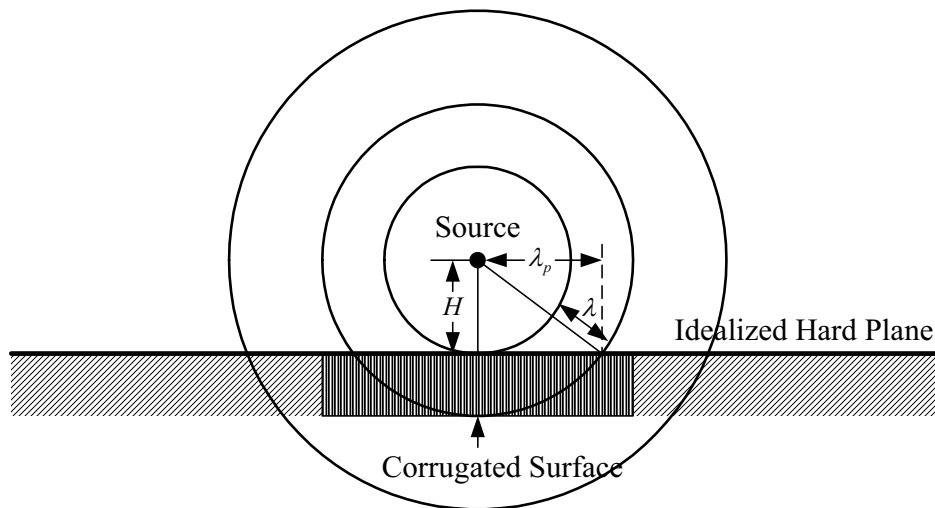


**Figure 23. Effective extension of the corrugation**

that of lower elevation angles, or that in the lateral direction, is strongly affected. This explains fairly well the phenomena.

The more quantitative explanation is shown in Figure 23. The wave front for a two-dimensional point source is circular, and different phase velocities are observed in different directions. In the radial direction from the source, the phase velocity is the normal acoustic velocity as is often used. In the direction along the ground surface, however, the phase velocity is generally different from the acoustic velocity. To be specific, generally the former is larger than the latter. For a source infinitely far away from the ground surface, or equivalently, for an incident plane wave, the phase velocity is infinitely large along the ground surface. If the phase velocity is defined as  $V_p = \lambda_p / T$ , where  $T$  is the period, it is seen that the associated wavelength  $\lambda_p$  also tends to infinity when the source height is extremely large. The effective extension of grooves is thus introduced as  $L_e = L / \lambda_p$ . It is readily obtained that  $\lambda_p = \lambda \sqrt{1 + 2H/\lambda}$ . Obviously, the larger the source height, the smaller the effective groove extension. When the source is right on the surface, i.e.,  $H = 0$ , so  $\lambda_p = \lambda$ , then the effective extension  $L_e = L / \lambda$ , achieving its maximum; while when the source is extremely far away, or,  $H \rightarrow \infty$ , then  $\lambda_p \rightarrow \infty$ , and  $L_e \rightarrow 0$ , that is, there is almost no contribution from the corrugation.

Physically, it is saying that the distance traveled by the acoustic wave in the high impedance part of the surface becomes shorter when the source is higher, and the total impedance thus becomes smaller, so the pressure decays slower. In other words, increasing the source height leads to the decrease of the lateral surface impedance. To maintain the desired high lateral impedance, the number of grooves needs to be increased to enlarge the corrugation extension. Considering that the noise spectrum is broadband, to sufficiently suppress the higher frequency components, a large number of grooves needs to be deployed because for the higher frequency, the source is of acoustically larger height though its physical height remains the same.

## VI. Conclusion

In this research, the physical grounds of impedance surface is first discussed. For a one-dimensional periodic structure such as a corrugated surface, transmission line is used to explain the underlying physics. When the groove size is much smaller than the wavelength, only leading

guided mode is propagating. If the groove is one-quarter wavelength deep, the open-circuit at the bottom is transformed into short circuit at the top.

For a more general case, such as a two-dimensional periodic structure, Helmholtz resonator turns out to be a suitable model when the wavelength is much larger than any dimension of the system. The occurrence of resonance corresponds to when the corrugated surface presents a low impedance or behaves like a soft surface. The resonance frequency is naturally associated with a frequency band within which the propagation of acoustic wave along surface is prohibited. The bandwidth is described using quality factor, which is a function of the geometry of grooves, implying that the system response can be tuned by adjusting the size and shape of grooves.

Two kinds of integral equation methods are proposed. One is based on the whole space or free space Green's function, the unknowns distributed along the groove walls and bottoms and the untextured surface. MLFMA is used to speed up the matrix-vector product entailed in the iterative method in solving the resultant linear system. The second is based on two half-space Green's functions by which a Neumann-Dirichlet map or an impedance boundary is introduced along the groove openings. The use of new Green's functions and impedance boundary ensures that the unknowns are distributed only over the openings, leading to substantial reduction in problem size.

How the geometry of grooves affects the wave propagation is studied quantitatively with the two integral equation methods. For the one-dimensional structure studied in the project, it turns out that the depth of one-quarter wavelength is necessary to achieve an artificial soft surface. The other prerequisite is that the opening is much smaller than the wavelength, ensuring that only leading guided mode is propagating so that a high impedance at the bottom is turned into a low impedance at the top. If the source is close to the surface, it turns out that about fifty grooves with openings of  $0.1\lambda$  are sufficient to make an artificial soft surface. Considering the engineering requirement, the opening is preferred to be made as small as possible. However, the effect on the wave propagation is decreased when the opening is made small, then the number of grooves has to be increased to balance the situation.

The noise spectrum generated by gun blast is generally of a band-limited structure. It is expected that the noise band and the forbidden band of the quasi-periodic structure overlap each other, so all noise components are disallowed to travel a large distance along the surface. It

turns out, however, that basically the resonance is very sensitive to the groove geometry so the forbidden band is generally narrow. One possible way is to use several grooves of different sizes. Numerical experiment shows that such a structure indeed expands the forbidden band of the system. The other way is to use a groove with a narrow neck and a large cavity, that is, a structure like a kettle, which, according to the prediction from the Helmholtz resonator, can lower the quality factor, and so can expand the forbidden band.

Experiment shows that source height also has a strong effect on the radiation pattern. The first influence is that, with the increase of height, the radiation pattern becomes more complicated, which is manifested by more and more nulls and peaks taking place. The second influence is that the effect of textured surface becomes weaker when the source moves away from the surface, entailing that the number of grooves be increased to balance the unfavorable tendency.

## References

Chew, W.C., ECE431 notes, University of Illinois at Urbana-Champaign, Urbana, Illinois, 2002.

Chew, W.C., J.-M. Jin, E. Michielssen and J. Song, Fast and Efficient Algorithms in Computational Electromagnetics, Artech House, Boston and London, 2001

Collin, R.E., Field Theory of Guided Waves, 2<sup>nd</sup> Edition, Wiley-IEEE Press, New York, 1990.

Kinsler, L.E., A.R. Frey, A.B. Coppens and J.V. Sanders, Fundamentals of Acoustics, 4<sup>th</sup> Edition, John Wiley & Sons, New York, 2000

Kong, J.A., Electromagnetic Wave Theory, EMW Publishing, Cambridge, Massachusetts, 1998.

Lam, Y.W., "A boundary integral formulation for the prediction of acoustic scattering from periodic structures," *J. Acoust. Soc. Am*, v. 105, pp. 762-769, 1999.

Qian, Y. , D. Sievenpiper, V. Radisic, E. Yablonovitch and T. Itoh, "A novel approach for gain and bandwidth enhancement of patch antennas," *IEEE Radio and Wireless Conference Dig.*, p. 221, Colorado Springs, CO, Aug. 1998.

Sievenpiper, D., L. Zhang, R.F.J. Broas, N.G. Alexópoulos and E. Yablonovitch, "High\_impedance electromagnetic surfaces with a forbidden frequency band," *IEEE Transactions on Microwave Theory and Techniques*, v. 47, pp. 2059-2074, 1999.

Swenson, G.W. Jr., E.R. Sandeen, L.L. Pater, and H.C. Zhuang, "The potential for mitigation of gun blast noise through sheltering of the source," USACERL Technical Report N-92/09, April 1992.

